

Comments on the radial distribution of charged particles in a magnetic field

H. Backe¹,

*Johannes Gutenberg-University Mainz, Institute for Nuclear Physics,
D-55099 Mainz, Germany*

Abstract

Magnetic guiding fields in combination with energy dispersive semiconductor detectors have been employed already more than 50 years ago for in-beam internal conversion electron spectroscopy. Even then it was recognized that efficiency modulations may appear as function of the electron energy, arising when electrons hit a baffle or miss the sensitive area of the detector. Current high precision beta decay experiments of polarized neutrons with conceptional similar experimental devices resulted in a detailed study of the point spread function (PSF). The latter describes the radial probability distribution of mono-energetic electrons at the detector plane. Singularities occur as function of the radial detector coordinate which have been investigated and discussed by Sjøe et al. (Rev. Scient. Instr. 86, 023102 (2015)), and Dubbers (arXiv:1501.05131v1 [physics.ins-det]). In this comment a rather precise numerical representation of the PSF is presented and compared with approximations in the mentioned papers.

Keywords: Charged particles in magnetic fields

1. Introduction

In two recent papers [1, 2] the radial spread of charged particles moving in a solenoidal magnetic guiding field has been investigated. The physical back-

¹corresponding author; E-Mail: backe@kph.uni-mainz.de

ground behind this attempt is based on the fact that the distribution of the
 5 particles at a detector with finite radius is a potential source of systematic er-
 rors in high precision experiments. To the latter belongs the measurement of
 the beta asymmetry in the decay of polarized neutrons, see, e.g., Ref. [3]. In
 principle, this fact is known since long. In the late 60th of the last century
 nuclear spectroscopists developed solenoidal transport systems, equipped with
 10 Si(Li) detectors as energy dispersive elements, for in-beam internal conversion
 electron spectroscopy. It was pointed out already in one of the first publications
 in detail [4] that the phase relation between polar emission angle and the radial
 coordinate at a circular Si(Li) detector, or a baffle between target and detector,
 results in unwanted fluctuations of the transmission probability as function of
 15 the electron energy. Efficiency modulations on the 10 % level were reported,
 e.g., in Ref. [5]. In order to overcome this problem, the unwanted wiggles were
 averaged out by wobbling the magnetic field strength, see, e.g., also Ref. [6, 7].

From the work of Sjøue et al. [1] and Dubbers [2] it is now well known
 that such efficiency modulations originate from singularities which appear in
 20 the so-called mono-energetic point spread function (PSF) as function of the
 radius coordinate. These singularities have been mathematically treated in the
 mentioned papers by means of different approaches. The probability density at
 the detector plane is presented by Sjøue et al. with the aid of an integral equation
 while explicitly by Dubbers, cf. Eq. (14) [1] and Eq. (12) [2], respectively. The
 25 ways to find solutions are quite different. Sjøue et al. solve the integral equation
 numerically, while Dubbers presents and discusses analytical approximations.

This contribution describes an alternative approach with which numerical
 solutions of arbitrary accuracy for the PSF can be obtained. It is based on the
 mathematically correct parameter representation of both, the radius coordinate
 30 $R(\cos\theta)$ and the probability density $dP(\cos\theta)/dR$ at the detector plane. Pa-
 rameter is $\cos\theta$ which intrinsically is a function of the polar emission angle θ
 at the source. Notice that for rotational symmetry $d(\cos\theta)$ is just proportional to
 the solid angle element $d\Omega$. In the next section 2 first some mathematical details
 are described. Results will be compared in section 3 with those presented in

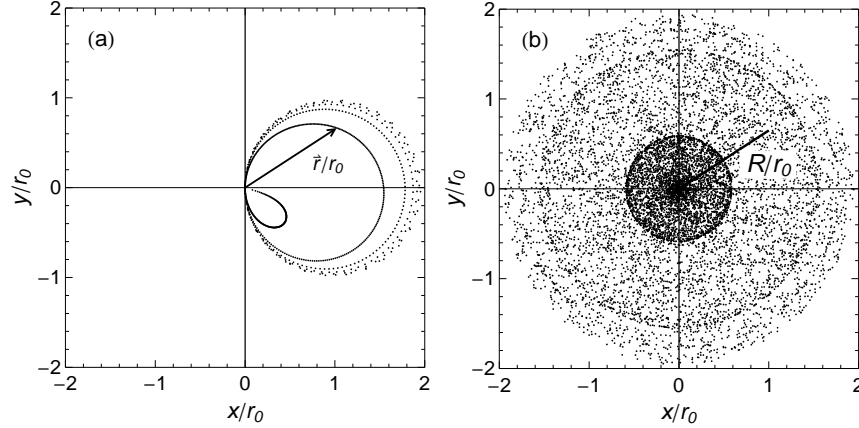


Figure 1: (a) Impact loci curve at the detector plane for polar emission angle variations in the interval $1 \geq \cos \theta \geq 0.2$ with decrements $\Delta \cos \theta = 0.001$. It is called in the text trajectory. Azimuthal emission angle $\varphi = 0$. (b) Scatter plot for $\cos \theta$ and φ randomly distributed. Parameters of Ref. [1] taken: $B = 0.326$ Tesla, $pc = 0.976$ MeV, $r_0 = p/(eB) = 0.01$ m, $z_0 = 0.10$ m, and $z_0/r_0 = 10$.

35 Ref. [1, 2]. The paper closes with conclusions in section 4.

2. Radial distribution at the detector plane

For the sake of convenience the nomenclature of Sjue et al., [1] will be adapted in the following. A right-handed coordinate system is defined with the magnetic field \vec{B} coinciding with the \hat{z} direction. The detector is placed
 40 in the (x,y) plane at a distance z_0 from the origin of the coordinate system in which the point source is located. The charged particle starts with polar angle θ and azimuthal angle φ , the latter defined with respect to the y axis. The point of impact at the detector plane is given by [1, Eq. (4)]

$$\frac{\vec{r}}{r_0} = \sqrt{1 - \cos^2 \theta} \left\{ \hat{x} \left[\left(1 - \cos \left(\frac{z_0}{r_0 \cos \theta} \right) \right) \cos \varphi + \sin \left(\frac{z_0}{r_0 \cos \theta} \right) \sin \varphi \right] + \right. \\ \left. + \hat{y} \left[- \left(1 - \cos \left(\frac{z_0}{r_0 \cos \theta} \right) \right) \sin \varphi + \sin \left(\frac{z_0}{r_0 \cos \theta} \right) \cos \varphi \right] \right\} \quad (1)$$

with $r_0 = p/(q \cdot B)$ the maximum projected orbital radius, p the momentum,
 45 and q the charge of the particle. Fig. 1 (a) depicts the loci the radius vector

\vec{r}/r_0 traverses according to Eq. (1) if the cosine of the polar emission angle θ is decremented in steps $\Delta \cos \theta = 0.001$. This impact loci curve must be distinguished from the projected orbit of the electron on its way from the target to the detector and will be called in the following trajectory.

50 The radius coordinate in the (x,y) plane reads [1, Eq. (12)]

$$\frac{R(\cos \theta)}{r_0} = \sqrt{\left(\frac{x}{r_0}\right)^2 + \left(\frac{y}{r_0}\right)^2} = \sqrt{2(1 - \cos^2 \theta) \left(1 - \cos\left(\frac{z_0}{r_0 \cos \theta}\right)\right)}. \quad (2)$$

The differential probability dP_c per normalized differential radius interval $d(R/r_0)$ is

$$\frac{dP_c(\cos \theta)}{dR/r_0} = \frac{dP_c(\cos \theta)}{d \cos \theta} \cdot \frac{d \cos \theta}{d(R/r_0)} = \frac{dP_c/d \cos \theta}{d(R/r_0)/d \cos \theta}. \quad (3)$$

For the example of an isotropically emitting source with $dP(\cos \theta)/d \cos \theta = 1$ and $d(R/r_0)/d \cos \theta$ calculated from Eq. (2) one obtains after some algebraic
55 manipulations

$$\frac{dP_c(\cos \theta)}{dR/r_0} = \frac{r_0 \cos^2 \theta \sqrt{1 - \cos^2 \theta}}{\left| (1 - \cos^2 \theta) z_0 \cos\left(\frac{z_0}{2r_0 \cos \theta}\right) + 2r_0 \cos^3 \theta \sin\left(\frac{z_0}{2r_0 \cos \theta}\right) \right|}, \quad (4)$$

or normalized to the unit area

$$\frac{dP_c(\cos \theta)}{dA} = \frac{1}{2\pi R r_0} \frac{dP_c(\cos \theta)}{dR/r_0}. \quad (5)$$

It can be shown that Eq. (5) agrees with Eq. (14) of Ref. [2].

Treating $\cos \theta$ as a free parameter, both the radial detector coordinate $R(\cos \theta)$ and $dP_c(\cos \theta)/dR$ can be calculated with Eq. (2) and (4), respectively. If the
60 parameter $\cos \theta$ is varied within the interval $\{1,0\}$ one gets an impression how $dP_c/d(R/r_0)$ evolves as function of R/r_0 . A corresponding parametric plot is depicted in Fig. 2 (a). Shown are branches which start at $R/r_0 = 0$ and end again at $R/r_0 = 0$ for each closed trajectory at the detector plane depicted in Fig. 1 (a). However, what is wanted, is the sum of all individual contribution
65 for a chosen normalized radius R/r_0 . This is the sum

$$\frac{dP(R/r_0)}{dR/r_0} = \sum_{n=m}^{\infty} \left(\frac{dP_c(\cos \theta|_n^>)}{dR/r_0} + \frac{dP_c(\cos \theta|_n^<)}{dR/r_0} \right) \quad (6)$$

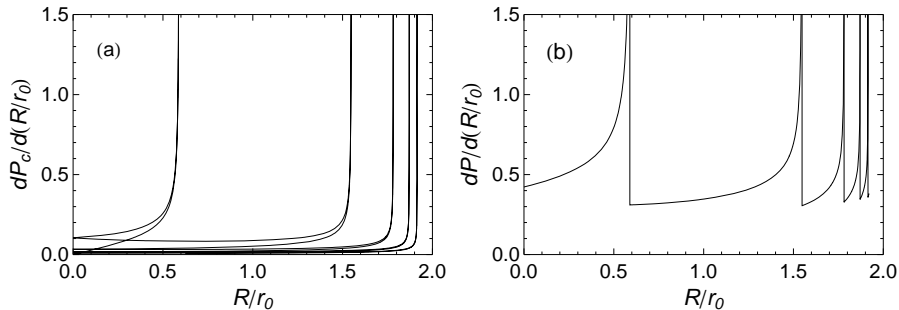


Figure 2: (a) Parametric representation of the differential probability $dP_c/(dR/r_0)$ as function of the normalized radius coordinate R/r_0 . The parameter $\cos \theta$ has been varied in the interval $\{1, 0.27\}$, i.e. 73 % of the emitted intensity has been exhausted. For $\cos \theta = 1$ the curve starts at the origin, evolves with decreasing $\cos \theta$ to the first spike which corresponds to the largest radius of the inner trajectory in Fig. 1 (a), returns to $R/r_0 = 0$ and evolves from there to the next spike. (b) Sum of 500 trajectories as function of the the normalized radius coordinate R/r_0 . Magnetic field and geometrical parameters the same as quoted in Fig. 1.

with $\cos \theta|_n^>$ and $\cos \theta|_n^<$ the two solutions of the equation

$$\sqrt{2(1 - \cos^2 \theta) \left(1 - \cos \left(\frac{z_0}{r_0 \cos \theta} \right) \right)} = \frac{R}{r_0} \quad (7)$$

for the n^{th} trajectory in the interval

$$\frac{z_0}{r_0 2\pi(n + n_f)} < \cos \theta \leq \min \left[\frac{z_0}{r_0 2\pi(n - 1 + n_f)}, 1 \right], \quad (8)$$

and $n_f = \text{floor}(z_0/(r_0 2\pi))$. The lower limit of the summation m is the smallest integer for which $R/R_n > 1$ holds with R_n the maximum radius of the n^{th} trajectory in the interval defined by the inequality (8).
70

3. Results and Discussion

In Fig.2 (b) numerical results on the basis of Eq. (6) are depicted. Totally 500 trajectories at the detector plane of Fig. 1 (a) have been taken into account. The accuracy of the calculation at $R/r_0 = 1.92$ and $R/r_0 = 0.6$ has been
75 estimated to be in the order of 1.8 %, and 0.6 %, respectively. The accuracy can be improved by extending the summation in Eq. (6) over more trajectories.

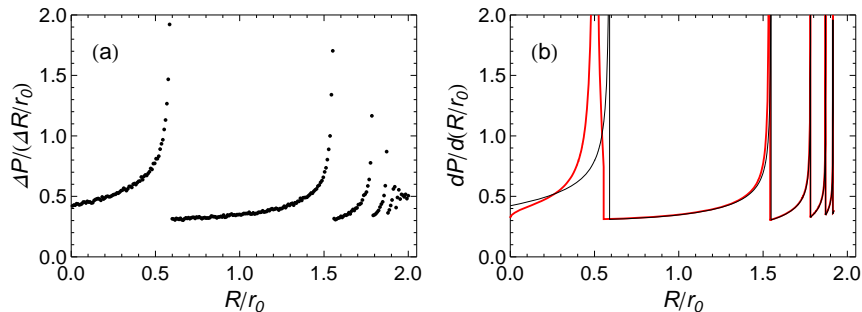


Figure 3: (a) Random distribution as shown in Fig. 1 (b) analyzed at the detector plane with a radial resolution of 0.8 % or for the treated example of 80 μm . (b) Comparison of the numerical true PSF of Dubbers [2] with the approximations presented in chapter 3 in red with the exact solution in black.

However, it should be mentioned that the series expansion Eq. (6) converges rather slowly.

In the interval $1.92 < R/r_0 \leq 2$ infinitely many spikes appear. It is not
 80 necessary to treat them in a mathematically exact manner. This fact is demonstrated in Fig. 3 (a). A number of 10^6 impact points at the detector plane were generated by randomly distributing $\cos \theta$ and φ in Eq. (1). A small sample is shown in Fig. 1 (b). The generated distribution has been analyzed with an
 85 virtual detector of 0.8 % spatial resolution in radial direction, corresponding for the chosen example with $r_0 = 1 \text{ cm}$ to 80 μm . It can clearly be seen that all the spikes in the mentioned interval result in a mean converging against 0.5. It should be mentioned that the same argument holds more or less for a finite beam spot size of the same order of magnitude. Fig. 3 (a) is fully in accord with Fig. 4 of Sjue et al. [1]. Probably the procedure applied by the authors to
 90 generate their Fig. 4 was nothing else than what has been just described here.

In Fig. 3 (b) the exact results are compared with the approximations elaborated by Dubbers [2]. In due distance from the spikes and for outer trajectories in Fig. 1 (a) with many revolutions, his approximation apparently seems to be rather good. For the important inner trajectory the approximation is rather
 95 poor, and even normalization is not preserved.

Finally the question should be addressed whether the considerations on the PSF of Ref. [1, 2] can be applied for field configurations other than homogeneous ones. It has been pointed out by Dubbers [2, ch. 5] that in axially symmetric, continuously descending magnetic fields the general formulas remain valid after replacement of R by $R \cdot \sqrt{B(z_0)/B(0)}$ with $B(0)$ and $B(z_0)$ the magnetic fields on-axis at the source and detector position, respectively. It is certainly true that the underlying adiabatic invariance considerations makes some valuable statements on the movement of charged particles in inhomogeneous magnetic fields [8, p. 592f], see also Ref. [5]. However, whether in the fundamental Eq. (2) the phase $z_0/(r_0 \cos \theta)$ of the cosine function can simply be replaced by $\sqrt{B(0)B(z_0)} z_0/[(B\rho)_p \cos \theta]$, with $(B\rho)_p = p/q$, maintaining otherwise the functional dependence is questionable and needs to be discussed in terms of quantitative accuracy considerations. For more general magnetic field configurations it seems unlikely to find analytical solutions equivalent to Eq. (2) and (4) and experimentalists would be well advised to investigate their instruments from the beginning by Monte-Carlo simulations performed with exact orbit calculations.

4. Conclusions

A method has been described with which mono-energetic point spread functions can be calculated with arbitrary accuracy for a homogeneous magnetic guiding field. It has been shown by Monte-Carlo simulations that a finite detector resolution or a finite target spot size smear out the singularities for trajectories in the detector plane originating from polar emission angles approaching $\theta = \pi/2$. The results of Sjue et al. [1] are fully in accord with the results obtained in this paper. Although Dubbers [2] presents the correct parameter representation for the probability density function, which is not explicitly quoted by Sjue et al. [1], his analytical approximations for the singularities appear for the innermost trajectories to be rather inaccurate with even a significant violation of the normalization.

125 In any case, the subject addressed in Ref. [1, 2] is appealing and certainly
beneficial for intuitional and educational purposes.

Acknowledgements

Calculations have been performed with the Wolfram Mathematica8.0 pack-
age. Pictures were prepared with the LevelScheme scientific figure preparation
130 system by M. A. Caprio, Department of Physics, University of Notre Dame,
Version 3.53 (January 10, 2013) [9].

References

References

- [1] S. K. L. Sjue, L. J. Broussard, M. Makela, L. McGaughey, A. R. Young, B. A.
135 Zeck, Radial distribution of charged particles in a magnetic field, Review of
Scientific Instruments 86 (2015) 023102 (6 pp).
- [2] D. Dubbers, Magnetic guidance of charged particles, arXiv:1501.05131v1
[physics.ins-det] (2015) 16 pp.
- [3] D. Dubbers, L. Raffelt, B. Märkisch, F. Friedl, H. Abele, The point spread
140 function of electrons in a magnetic field, and the decay of the free neutron,
Nuclear Instruments and Methods A 763 (2014) 112–119.
- [4] B. Klank, R. A. Ristinen, Design and Performance of a Transport Solenoid
- Si(Li) Detector Conversion Electron Spectrometer for On-Line Use with
Accelerators, in: J. H. Hamilton, J. C. Manthuruthil (Eds.), Radioactiv-
145 ity in Nuclear Spectroscopy, Modern Techniques and Applications, Vol. I,
Proceedings of the International Conference on Radioactivity in Nuclear
Spectroscopy (Vanderbilt University) (1969).
- [5] K. Kotajima, R. Beringer, A Magnetic Solenoid Electron Transporter, The
Review of Scientific Instruments 41 (1970) 632–635.

- 150 [6] Th. Lindblad, C. G. Lindén, An On-line Multichannel Electron Spectrometer
with High Transmission, *Nuclear Instruments and Methods* 126 (1975) 397–
406.
- [7] H. Backe, L. Richter, R. Willwater, E. Kankeleit, E. Kuphal, Y. Nakayama,
B. Martin, In-Beam Spectroscopy of Low Energy Conversion Electrons with
155 a Recoil Shadow Method - A New Possibility for Subnanosecond Lifetime
Measurements, *Zeitschrift für Physik A* 285 (1978) 159–169.
- [8] J. D. Jackson, *Classical Electrodynamics*, 3rd Edition, John Wiley & Sons,
Inc., New York, Chichester, Weinheim, Brisbane, Singapore, Toronto.
- [9] M. A. Caprio, LevelScheme: A level scheme drawing and scientific figure
160 preparation system for Mathematica, *Computer Physics Communications*
171 (2005) 107–118.